THE SZEWALSKI INSTITUTE OF FLUID-FLOW MACHINERY
POLISH ACADEMY OF SCIENCES

TRANSACTIONS OF THE INSTITUTE OF FLUID-FLOW MACHINERY

116

WYDAWNICTWO IMP PAN

GDAŃSK 2005

TRANSACTIONS OF THE INSTITUTE OF FLUID-FLOW MACHINERY

Appears since 1960

Aims and Scope

Transactions of the Institute of Fluid-Flow Machinery have primarily been established to publish papers from four disciplines represented at the Institute of Fluid-Flow Machinery of Polish Academy of Sciences, such as:

- Liquid flows in hydraulic machinery including exploitation problems,
- Gas and liquid flows with heat transport, particularly two-phase flows,
- Various aspects of development of plasma and laser engineering,
- Solid mechanics, machine mechanics including exploitation problems.

The periodical, where originally were published papers describing the research conducted at the Institute, has now appeared to be the place for publication of works by authors both from Poland and abroad. A traditional scope of topics has been preserved.

Only original and written in English works are published, which represent both theoretical and applied sciences. All papers are reviewed by two independent referees.

EDITORIAL AND PUBLISHING OFFICE

IFFM Publishers (Wydawnictwo IMP), The Szewalski Institute of Fluid Flow Machinery, Fiszera 14, 80-952 Gdańsk, Poland, Tel.: +48(58)3411271 ext. 141, Fax: +48(58)3416144, E-mail: esli@imp.gda.pl http://www.imp.gda.pl/

Terms of subscription

Subscription order and payment should be directly sent to the Publishing Office

Warunki prenumeraty w Polsce

Wydawnictwo ukazuje się przeciętnie dwa lub trzy razy w roku. Cena numeru wynosi 20,- zł + 5,- zł koszty wysyłki. Zamówienia z określeniem okresu prenumeraty, nazwiskiem i adresem odbiorcy należy kierować bezpośrednio do Wydawcy (Wydawnictwo IMP, Instytut Maszyn Przepływowych PAN, ul. Gen. Fiszera 14, 80-952 Gdańsk). Osiągalne są również wydania poprzednie. Prenumerata jest również realizowana przez jednostki kolportażowe RUCH S.A. właściwe dla miejsca zamieszkania lub siedziby prenumeratora. W takim przypadku dostawa następuje w uzgodniony sposób.

Articles in *Transactions of the Institute of Fluid-Flow Machinery* are abstracted and indexed within:

INSPEC Database;
Energy Citations Database;
Applied Mechanics Reviews;
Abstract Journal of the All-Russian Inst. of Sci. and Tech. Inf. VINITI.

ISSN 0079-3205

TRANSACTIONS OF THE INSTITUTE OF FLUID-FLOW MACHINERY

No. 116, 2005, 71-89

ANDRZEJ BŁASZCZYK*

Numerical and experimental flow investigations in pump channel elements

Institute of Turbomachinery, Technical University of Lodz, 93-005 Lodz, Poland

Abstract

The results of numerical and experimental investigations of hydraulic system elements (an impeller and a vaned diffuser) of the selected pump have been presented. The code [5, 8] that solves the three-dimensional viscous flow of a compressible and incompressible fluid and that has been developed at the Institute of Turbomachinery, Technical University of Lodz has been employed in the numerical calculations. The experimental investigations of the selected pump type have been carried out on the test stand that allows, among others, for measurement of the working medium volume flow rate; measurement of power and frequency of rotations and measurement of local pressures in selected control planes and points.

Keywords: Pump; Numerical analysis; Experimental analysis; Flow structure; CFD

Nomenclature

b	–	channel width
c	–	absolute velocity
D	–	diameter or the function of dissipation
H	–	total head
$\Im$	–	Jakobian
l	–	blade length measured along the blade camber line arc, gap length
p	–	pressure
$\nu^i, \nu^j, \nu^k, \nu^n$	–	contravariant velocity components

*E-mail address: akblaszc@mail.p.lodz.pl

s	–	blade thickness
z	–	number of impeller blades, co-ordinate of the Cartesian co-ordinate system
z_k	–	number of vanes in the vaned diffuser
Q	–	discharge, volume flow rate
w	–	relative velocity
x^i	–	co-ordinates of the hydraulic system
α^*	–	slope angle of the vane camber line of the vaned diffuser
β	–	angle between u and w of the working medium stream
β^*	–	slope angle of the blade camber line
θ	–	angle in the polar co-ordinate system (circumferential direction)
μ_{ef}	–	effective dynamic viscosity
μ	–	coefficient of the blocking area
η	–	total efficiency of the pump
Δ	–	rise (occurs with the symbol of a given quantity)
ρ	–	density of the liquid pumped
τ^{ij}	–	stress tensor

Subscripts and superscripts

D	–	vaneless diffuser
h	–	hydraulic
K	–	vaned diffuser
KT	–	discharge nozzle
m	–	meridional
max	–	maximum
N	–	nominal
PW	–	water jacket
r	–	radial
s	–	losses
u	–	circumferential
up	–	front gap
W	–	impeller
t	–	pump outlet
0	–	impeller inlet
1	–	impeller blade wheel inlet
2	–	impeller outlet
3	–	inlet to the guide vanes
4	–	vaned diffuser outlet
5	–	water jacket outlet

All quantities are expressed in the fundamental units of the SI system.

1 Introduction

Impeller pumps belong to most commonly used machines. It is difficult to name all the branches of the national economy they have been applied in.

According to [4], 20÷30% of the electrical energy generated in individual countries is used to drive pumps. Other types of pump driving motors should be mentioned here as well, such as: steam turbines, internal combustion turbines, air turbines, combustion and hydraulic engines, whose share as the driving power of pumps is lower, but still significant.

Modern impeller pumps, especially those of high power, should be characterised by the maximum level of efficiency $\eta = \eta_{max}$ that can be achieved under present technological conditions, at the required performance parameters $H(Q)$ and $P(Q)$. It is connected with a need to optimise all elements of the pump stage during the designing process.

Such possibilities are offered by widely developed numerical methods for flow structure investigations in machine elements. These methods are at present used in analyses and qualitative evaluations of velocity and static pressure distributions in hydraulic passages of machines.

The sufficiently accurate calculation of the actual flow that occurs in turbomachines requires a numerical solution of the complete system of Navier-Stokes differential equations of motion. However, it is impossible now to design the optimal geometry of pump elements at the assumed parameters H, Q, n by means of this method.

At present, the process of designing and optimisation of pump hydraulic systems is carried out in two stages:

I. Determination of main dimensions of hydraulic passages with a method based on the one-dimensional flow model.

II. Analysis of local parameters of the working medium in pump hydraulic passages conducted with three-dimensional (3D) flow computational methods, with a possibility of correction of main dimensions.

The results of numerical calculations of the flow through the impeller and vaned diffuser channels of the selected pump type are presented and compared with the results of experimental investigations. This analysis results from the occurrence of these quantities in both stages of the pump designing process.

2 Hydraulic system of the pump

The pump hydraulic system consists of an impeller, a vaneless diffuser, a centrifugal vaned diffuser with a radial-axial flow, a water jacket being a cooler of the engine at the same time, and a discharge nozzle. A scheme of the hydraulic system is presented in Fig. 1.

The main dimensions of the impeller and the radial-axial vaned diffuser are presented in Tabs. 1 and 2, respectively.

The main dimensions have been established by means of one of the design methods based on the one-dimensional flow model. The values of hydraulic parameters of the impeller and the vaned diffuser determined with this method have

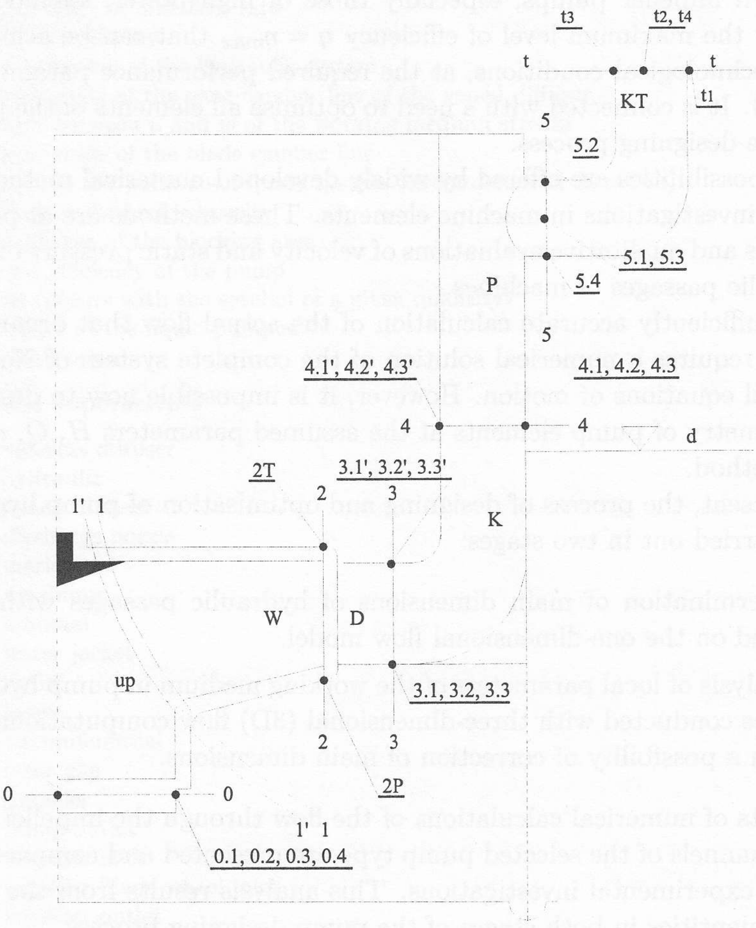

Figure 1. Scheme of the hydraulic system and the arrangement of holes for measurement of static pressures on pump channel walls. Notation: W – impeller, D – vaneless diffuser, K – radial-axial vaned diffuser, PW – water jacket, KT – discharge nozzle, d – level of the liquid in the tank, 0.1, 0.2, 0.3, 0.4 – ϕ 0.5 mm holes for static pressure measurements in the pump suction nozzle, 2P, 2T – ϕ 0.5 mm holes for the receipt of the static pressure signal in the impeller inlet cross-section, 3.1, 3.2, 3.3 – ϕ 0.5 mm holes for the receipt of the static pressure signal at the vaned 3.1′, 3.2′, 3.3′ diffuser inlet, 4.1, 4.2, 4.3 – ϕ 0.5 mm holes for the receipt of the static pressure signal at the vaned 4.1′, 4.2′, 4.3′ diffuser outlet, 5.1, 5.2, 5.3, 5.4 – ϕ 0.5 mm holes for static pressure measurements at the discharge nozzle inlet, t_1, t_2, t_3, t_4– ϕ 0.5 mm holes for static pressure measurements at the discharge nozzle outlet.

Table 1. Main dimensions of the impeller

IMPELLER													
1	2	3	4	5	6	7	8	9	10	11	12	13	14
D_0	D_1	b_1	s_1	β_1^*	D_2	b_2	s_2	β_2^*	z	l	D_{up}	b_{up}	l_{up}
[m]	[m]	[m]	[m]	[°]	[m]	[m]	[m]	[°]	-	[m]	[m]	[m]	[m]
0.085	0.08	0.061	0.00735	17	0.28	0.015	0.0175	11.5	3	0.44	0.115	0.0003	0.017

Table 2. Main dimensions of the diffuser

VANED DIFFUSER								
1	2	3	4	5	6	7	8	9
D_3	b_3	s_3	α_3^*	D_{4Z}	D_{4W}	s_4	α_4^*	z_k
[m]	[m]	[m]	[°]	[m]	[m]	[m]	[°]	-
0.32	0.024	0.005	9	0.42	0.3555	0.06	90	6

been shown together with the results of numerical calculations on the subsequent diagrams.

3 Determination of local parameters of the working medium flow through the pump with the three-dimensional calculation method

3.1 Basic equations

For the calculations of 3D flows in hydraulic passages of the impeller and the radial-axial vaned diffuser (Fig. 1), a code solving the 3D viscous flow of a compressible and incompressible fluid that has been developed at the Institute of Turbomachinery, Technical University of Lodz, has been employed. The theoretical basis and the calculation algorithm have been discussed in [5, 8]. The primary equations (Eqs. (1) and (2)) are formulated in the curvilinear system of co-ordinates and have the following form:

$$\frac{\partial}{\partial x^j}\left(\frac{\rho v^j}{\Im}\right) = 0; \tag{1}$$

$$\frac{\partial}{\partial x^j}\cdot\left(-\frac{\rho v^j v^n}{\Im} + \frac{\tau^{nj}}{\Im}\right) + \frac{1}{\Im}\Gamma^n_{ij}\left(-\rho v^i v^j + \tau^{ij}\right) + \frac{\rho f^n}{\Im} - \frac{g^{nk}}{\Im}\frac{\partial p}{\partial x^k} = 0; \quad n = 1,2,3 \tag{2}$$

where the centrifugal force and the Coriolis force in the curvilinear system equal:

$$f^n = |\omega|^2 r^n + 2\varepsilon^{njk}\omega_j \cdot v_k \Im \tag{3}$$

and the stress tensor is equal to:

$$\tau^{nj} = \mu_{ef}\left(g^{jk}\frac{\partial \nu}{\partial x^k} + g^{nk}\frac{\partial \nu}{\partial x^k} - \frac{\partial g^{nj}}{\partial x^k}v^k\right). \tag{4}$$

In the numerical calculations of flows through the selected hydraulic passages of the pump, an algebraic program of the Baldwin-Lomax model of turbulence has been applied [1]. In this program, the effective viscosity for the determination of stresses has been presented as a sum of the following components:

$$\mu_{ef} = \mu + \mu_T \tag{5}$$

where: μ – molecular viscosity, μ_T – turbulent viscosity.

A detailed description of the determination of the viscosity μ and μ_T is presented in [1].

3.2 Boundary conditions

The system of Eqs. (1) and (2) is an elliptic system of partial equations that requires the following boundary conditions to be posed:

- Velocity profile at the inlet to the computational domain; in each node of the computational grid, the respective velocity components are given on the inlet surface.
- Distribution and values of the static pressure at the calculation channel outlet (Fig. 2).
- Zero gradient of the static pressure at the calculation channel outlet.
- Velocity equal to zero on the calculation channel walls.
- Periodicity along the direction x^2 (the grid has been built in such a way as to make the co-ordinate x^2 correspond to the circumferential direction).

In the impeller and vaned diffuser passages under consideration, the following conditions have been assumed:

- Homogenous velocity profile without the circumferential component at the impeller inlet that results from the mass flow rate in the impeller.
- Identical value of the static pressure on the outlet surface, along the radius longer by 15% than the outer radius of the impeller. The individual velocity components at the impeller outlet have been averaged as follows:

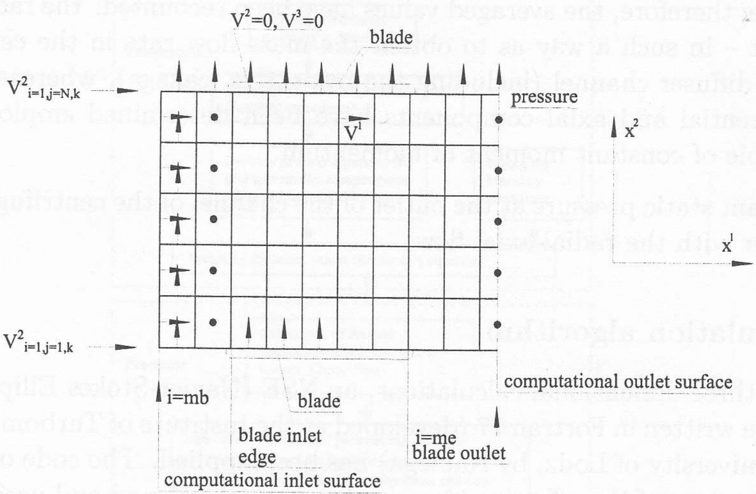

Figure 2. Assignment of the boundary values to the wall.

1. radial component has been averaged on the basis of the equation of mass flow rate, according to the following relationship:

$$\bar{c}_{2r}(z) = \frac{1}{2\pi} \int_{0}^{2\pi} c_{2r} d\theta \, ; \tag{6}$$

2. circumferential and axial components have been averaged, while maintaining the moment of momentum constant, according to the equations:

$$\bar{c}_{2u}(z) = \frac{1}{2\pi \bar{c}_{2r}} \int_{0}^{2\pi} (w_{2r} + u) \cdot c_{2r} d\theta \, , \tag{7}$$

$$\bar{c}_{2z}(z) = \frac{1}{2\pi \bar{c}_{2r}} \int_{0}^{2\pi} c_{2z} \cdot c_{2r} d\theta \, . \tag{8}$$

- Obtained velocity field of the medium flowing from the impeller along the radius equal to the inlet radius to the centrifugal vaned diffuser channel is the boundary condition at the inlet to the stationary passage of this vaned diffuser.
- Calculation inlet surface to the centrifugal vaned diffuser stationary channel was situated along the radius shorter by approx. 15% than the real inlet

surface; therefore, the averaged values have been recounted: the radial component – in such a way as to obtain the mass flow rate in the centrifugal vaned diffuser channel (including the respective leakage), whereas the circumferential and axial components have been determined employing the principle of constant moment of momentum.

- Constant static pressure at the outlet of the channel of the centrifugal vaned diffuser with the radial-axial flow.

3.3 Calculation algorithm

For the three-dimensional calculations, an NSE (Navier-Stokes Elliptic) software package written in Fortran 77 (developed at the Institute of Turbomachinery, Technical University of Lodz, by Rabiega) has been applied. The code of the calculation procedure of the effective viscosity has been developed and used, among others, in [3]. The procedures written by Rabiega and Papierski [7] in AutoLisp and operating in the AutoCAD graphical environment have been employed as the pre-processor.

These procedures allow one to generate a computational grid in an interactive way on the basis of the geometry drawn in AutoCAD. As the post-processor, the commercial TECPLOT software made by Amtec, which allows for the graphical presentation of the distributions of velocity and pressure fields, has been employed.

A block scheme of the calculations, quoted after [3], is presented below.

4 Results of numerical and experimental investigations

Below, the results of numerical and experimental investigations conducted for the selected P1 pump type are discussed.

The comparison between calculation and experimental results of hydraulic system elements (impeller, vaned diffuser) has been carried out in order to evaluate the posed boundary conditions in Eqs. (1) and (2), the assumed model of turbulence in the light of the two-stage designing process of the pump (Section 1).

The application of the results of numerical experimental investigations of only impellers and vane diffusers follows from the fact that they play a decisive role in the energy transfer to the flowing medium and in the exchange of the kinetic energy into the potential one (Fig. 3). The calculations have been carried out for three discharges, whose values are given on the diagram. The pump nominal discharge is equal to $Q_N = 0.04789$ m^3/s.

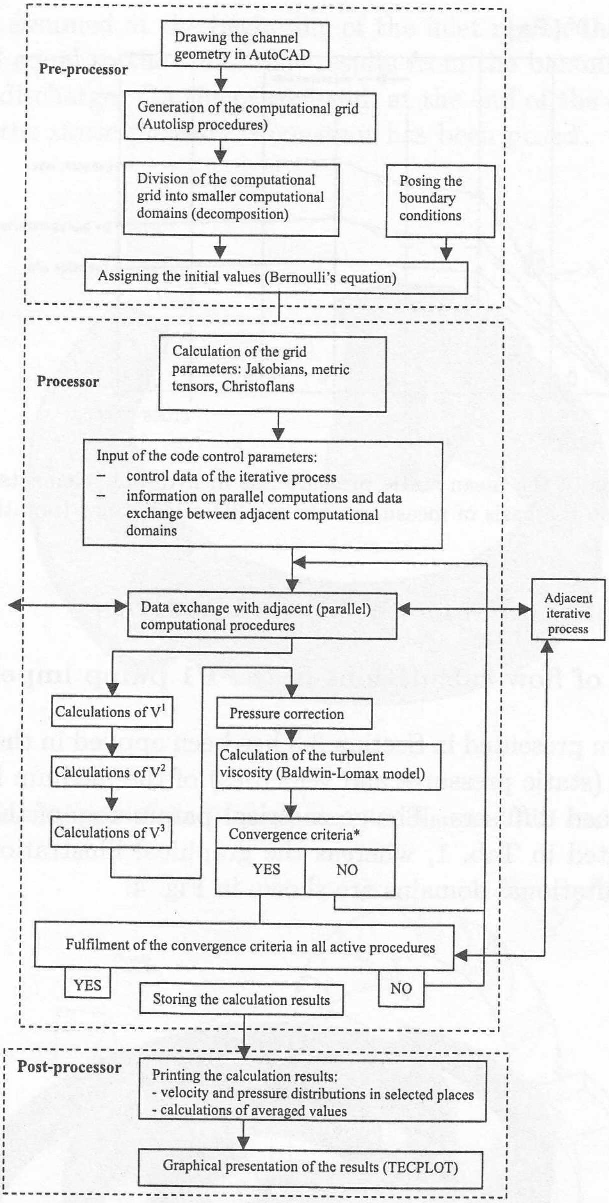

* Convergence criteria:

1. $\frac{\sum S^*_{mp}}{\dot{m}} < \varepsilon$, where: $\sum S^*_{mp}$ – sum of non-balanced mass flow rates in all control volumes, $\dot{m}$ – mass flow rate in the channel, $\varepsilon = 1e-5$ – arbitrarily assumed value;
2. $\frac{\max(\Delta V^i)}{V^i} < \varepsilon$, where: $\max\left(\Delta V^i\right)$ – maximum change in the ith contravariant velocity component during the iteration step, V^i – contravariant velocity component, $\varepsilon = 1e-4$ – arbitrarily assumed value;
3. $\frac{\max(\Delta\mu)}{\mu} < \varepsilon$, where: $\max(\Delta\mu)$ – maximum change in the dynamic viscosity, μ – dynamic viscosity, $\varepsilon = 1e-5$ – arbitrarily assumed value.

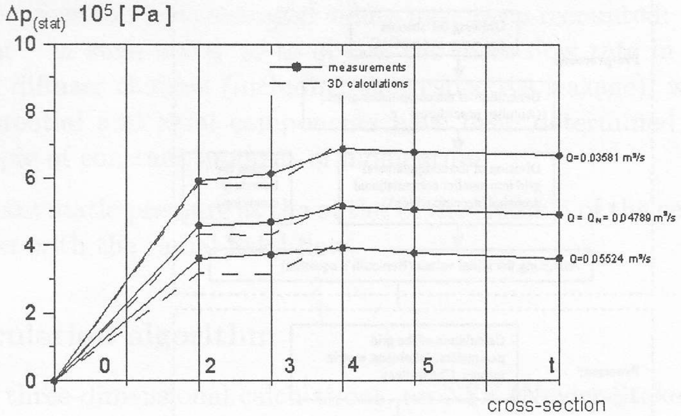

Figure 3. Comparison of the mean static pressure rise in hydraulic elements of the pump, determined on the basis of measurements and 3D calculations (notations as in Fig. 1).

4.1 Results of the numerical 3D flow analysis

4.1.1 Results of flow calculations in the P1 pump impeller

The algorithm presented in Section 3.3 has been applied in the calculations of local parameters (static pressures and velocities) of the medium flowing through impellers and vaned diffusers. The geometrical parameters of the PS pump impeller are presented in Tab. 1, whereas the graphical illustration and the inlet and outlet computational domains are shown in Fig. 4.

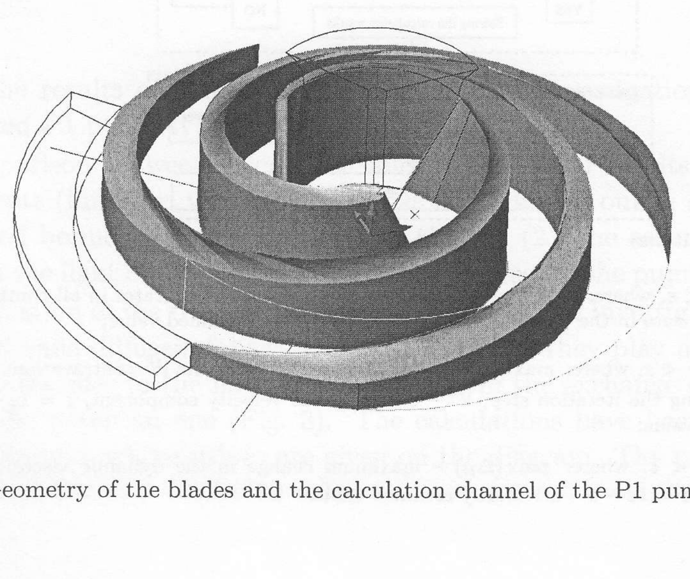

Figure 4. Geometry of the blades and the calculation channel of the P1 pump impeller.

It has been assumed at the beginning of the inlet region that the velocity c_0 is constant and equal to the value that results from the balance assumed in the calculations of discharge. On the other hand, at the end of the outlet region, the condition that the static pressure is constant has been posed.

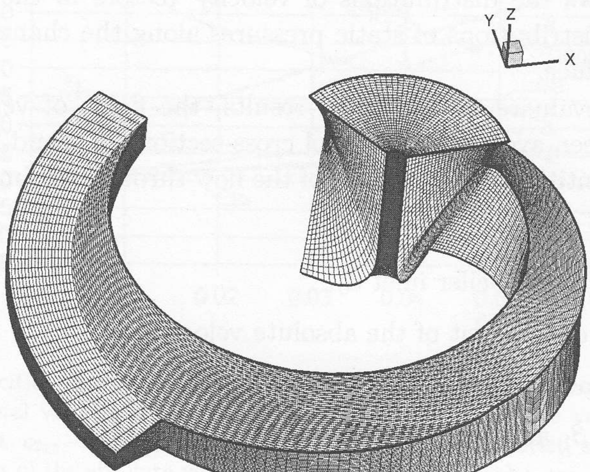

Figure 5. Computational grid of the P1 pump impeller channel. Grid size $x^1 = 140$, $x^2 = 41$, $x^3 = 31$.

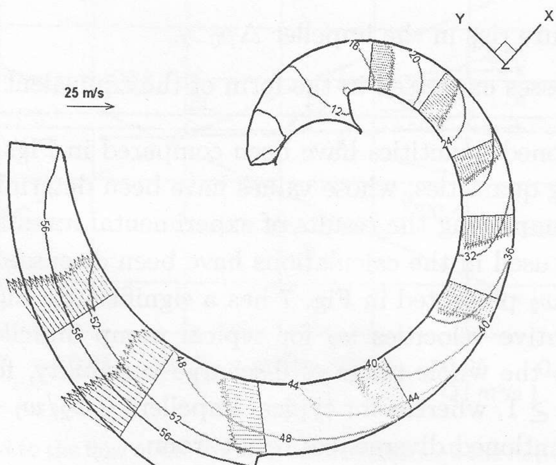

Figure 6. Distribution of relative velocities and static pressures on the mean stream surface of the P1 pump impeller. Nominal discharge.

The computational grid assumed for the selected impeller, together with the extended regions at the inlet and outlet, have been shown in Fig. 5. The outlet and inlet computational domains have been generated with the grid lines x^1 drawn along the radial direction, x^2 – along the circumferential direction, and x^3 – along the axial direction.

Figure 6 shows the distributions of velocity vectors in the selected control planes and the distributions of static pressures along the channel length for the mean stream surface.

In order to evaluate the obtained results, the fields of velocity and static pressures have been averaged in control cross-sections 0, 1 and 2 (Fig. 1). Thus, the averaged quantities, characteristic of the flow through the impeller, have been obtained, namely:

- velocity at the impeller inlet c_0,
- meridional component of the absolute velocity c_{1m},
- relative velocity w_1,
- inlet angle β_1 and the angle of incidence δ_1,
- relative velocity w_2,
- meridional component of the absolute velocity c_{2m},
- circumferential component of the absolute velocity c_{2u},
- outlet angle β_2,
- static pressure rise in the impeller Δp_{0-2},
- hydraulic losses expressed in the form of the equivalent pressure Δp_{sW}.

The above-mentioned quantities have been compared in Figs. 3, 7, 8 and 9 with the corresponding quantities, whose values have been determined on the basis of the calculations employing the results of experimental investigations.

The formulae used in the calculations have been discussed in [3].

The velocity w_2 presented in Fig. 7 has a significantly higher value than the values of the relative velocities w_2 for typical pump impellers. It should also be stated that in the whole range of discharge variability, for all pumps under analysis – $w_2/w_1 \geq 1$, whereas for typical impellers – $w_2/w_1 < 1$.

The above-mentioned divergences result from:

- high value of the velocity of transportation u_2,
- small outlet angle and a large inlet angle in the impeller; in the case of these pumps, always $\beta_1 > \beta_2$.

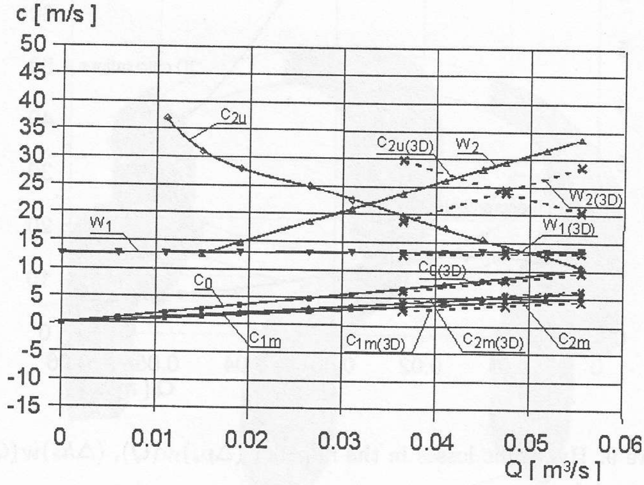

Figure 7. Flow velocities through the pump impeller: c_0 – velocity at the impeller inlet, c_{1m} – meridional velocity at the blade wheel inlet, w_1 – relative velocity at the blade wheel inlet, c_{2m} – meridional velocity at the blade wheel outlet, c_{2u} – circumferential component of the absolute velocity at the blade wheel outlet, w_2 – relative velocity at the impeller outlet (quantities with the subscript 3D refer to the results of numerical calculations).

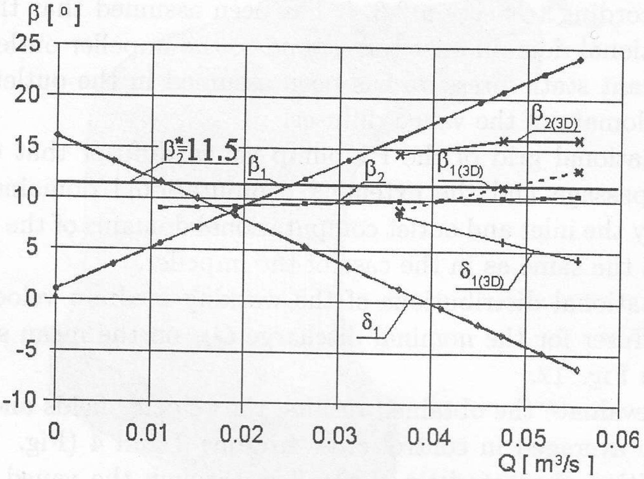

Figure 8. Angles related to the flow of the working medium through the impeller: β_1 – blade inlet angle, δ_1 – angle of incidence, β_2 – blade outlet angle (quantities with the subscript 3D refer to the results of numerical calculations), β_2^*– design angle of the blade at the impeller outlet.

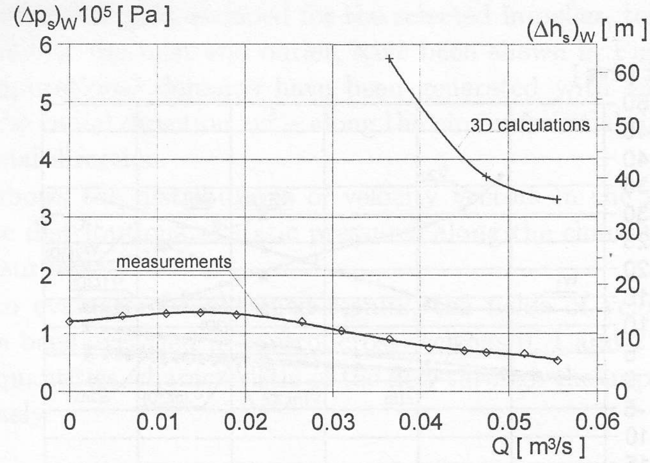

Figure 9. Hydraulic losses in the impeller $(\Delta p_s)_W(Q)$, $(\Delta h_s)_W(Q)$.

4.1.2 Results of flow calculations in the P1 pump vaned diffuser

The geometry of the vaned diffuser is presented in Tab. 2 and depicted in Fig. 10.

Also, this figure shows a calculation extension of the inlet and outlet region of one of passages in which the boundary conditions are posed for the calculations. In this case, according to Section 3.2, it has been assumed that the parameters at the computational domain inlet correspond to the impeller outlet parameters, whereas a constant static pressure has been assumed in the outlet plane of the computational domain of the vaned diffuser.

The computational grid of the P1 pump vaned diffuser that comprises the blade-to-blade passage and the extended computational domains is shown in Fig. 11. The way the inlet and outlet computational domains of the vaned diffuser are generated is the same as in the case of the impeller.

The computational distributions of the working medium velocity in the P1 pump vaned diffuser for the nominal discharge Q_N on the mean stream surface are presented in Fig. 12.

In order to evaluate the obtained results, the velocity fields and the pressure fields have been averaged in control cross-sections 3 and 4 (Fig. 1). Thus, the averaged quantities, characteristic of the flow through the vaned diffuser, have been determined. These are:

- meridional component of the velocity at the vaned diffuser inlet c_{3m},
- circumferential component of the velocity c_{3u},
- total velocity at the vaned diffuser outlet c_4,

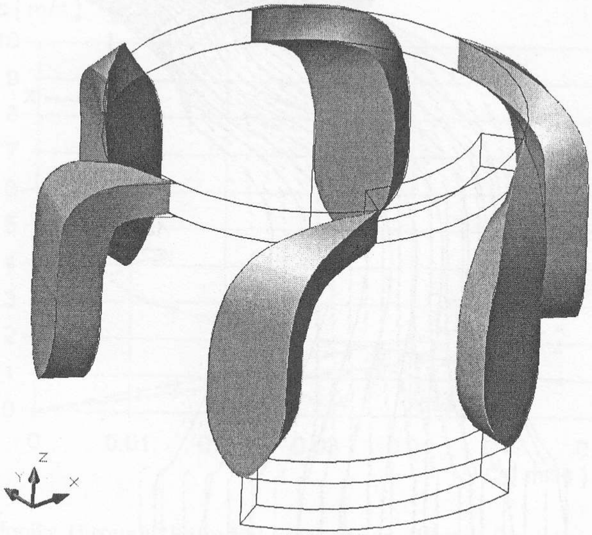

Figure 10. Geometry of the vanes and the calculation channel of the P1 pump vaned diffuser.

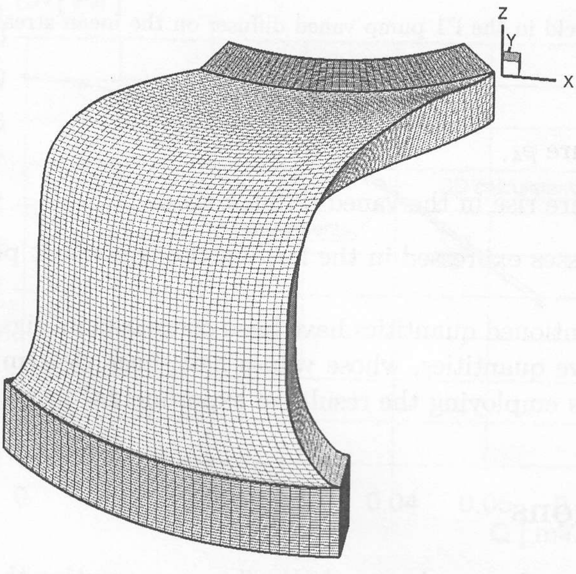

Figure 11. Computational grid of the P1 pump vaned diffuser channel. Grid size $x^1 = 136$, $x^2 = 41$, $x^3 = 21$.

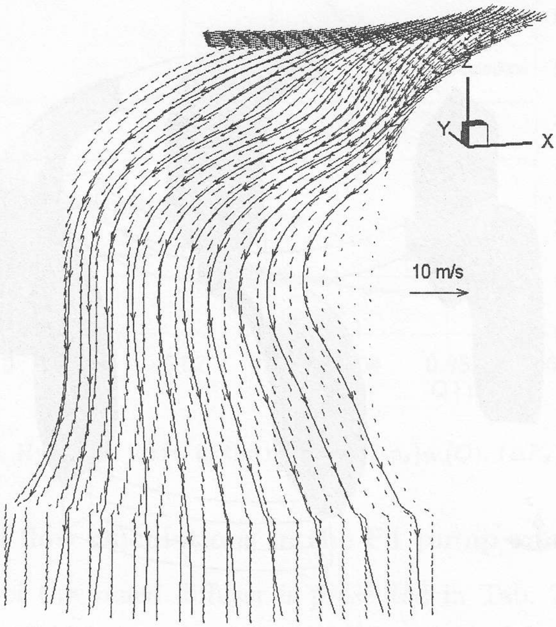

Figure 12. Velocity field in the P1 pump vaned diffuser on the mean stream surface. Nominal discharge.

- static pressure p_4,
- static pressure rise in the vaned diffuser Δp_{3-4},
- hydraulic losses expressed in the form of the equivalent pressure Δp_{sK}.

The above-mentioned quantities have been compared in Figs. 3, 13, 14 and 15 with the respective quantities, whose values have been determined on the basis of the calculations employing the results of experimental investigations.

5 Conclusions

The divergences that can be seen in the figures presenting the averaged results of experimental investigations and numerical calculations can be decreased when another model of turbulence is used and when the boundary conditions posed in the calculations are more precise.

The characteristic curves presenting:

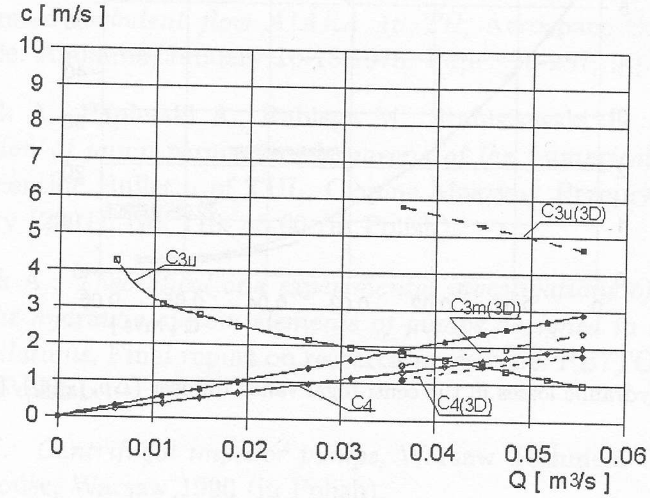

Figure 13. Flow velocity through the radial-axial vaned diffuser (quantities with the subscript 3D refer to the results of numerical calculations).

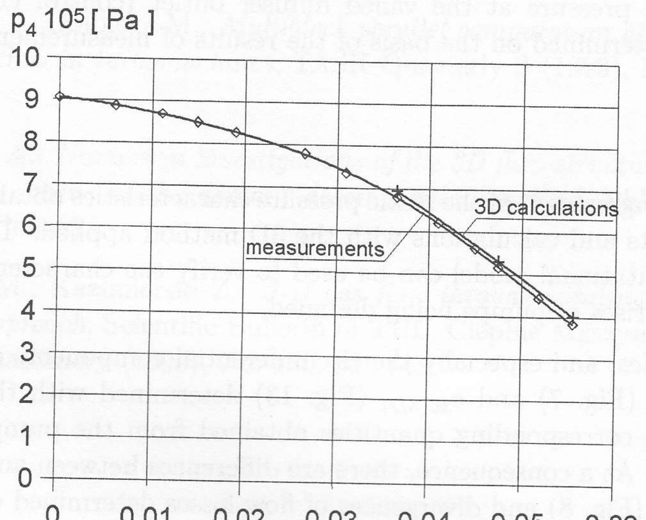

Figure 14. Characteristic curve representing the manometric static pressure at the vaned diffuser outlet $p_4(Q)$.

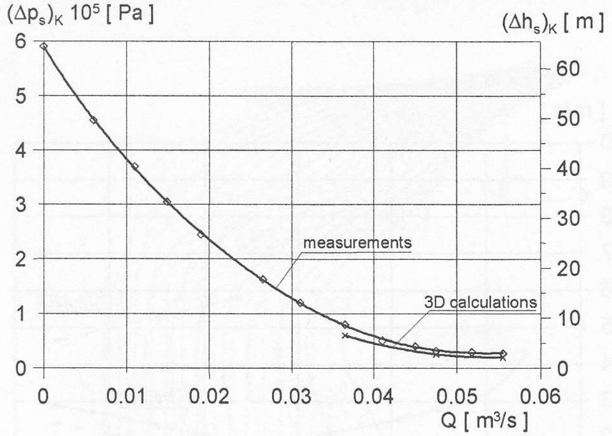

Figure 15. Hydraulic losses in the centrifugal vaned diffuser $(\Delta p_s)_K(Q)$, $(\Delta h_s)_K(Q)$.

1. the mean static pressure rise in pump hydraulic elements, which has been determined on the basis of measurements and 3D calculations (Fig. 3), and

2. the static pressure at the vaned diffuser outlet (control cross-section 4, Fig. 1) determined on the basis of the results of measurement and 3D calculations

confirm a good agreement of the static pressure characteristics obtained as a result of measurements and calculations with the 3D method applied. This means the assumed computational model can be used to verify the characteristic curves of static pressure rises of pumps being designed.

The velocities, and especially the circumferential components of absolute velocities $c_{2u(3D)}$ (Fig. 7) and $c_{3u(3D)}$ (Fig. 13) determined with the 3D method differ from the corresponding quantities obtained from the pump performance measurements. As a consequence, there are differences between angles $\beta_{1(3D)}$, β_1 and $\beta_{2(3D)}$, β_2 (Fig. 8) and divergences of flow losses determined on the basis of measurements and 3D calculations (Fig. 19). This means the assumed calculation model requires further improvements to be applied in performance calculations. At the present moment, it can be helpful in a qualitative analysis of the flow through pump hydraulic passages.

Received 10 March 2004

References

[1] Baldwin B.S., Lomax H.: *Thin layer approximation and algebraic model for separated turbulent flow AIARA 16 TH*, Aerospace Sciences Meeting Huntsville. Alabama/January 16-18.1978. Paper 78-257, 9 p., 13 refs.

[2] Błaszczyk A., Papierski A., Rabiega M., Staniszewski J.: *Method for determination of pump parameters by means of the numerical analysis of 3D flows*, Scientific Bulletin of TUL, Cieplne Maszyny Przepływowe – Turbomachinery (2001), No. 119, 45-60 (in Polish).

[3] Błaszczyk A.: *Theoretical and experimental investigations of the flow structure in the hydraulic system elements of pumps designed to operate in various installations*, Final report on research project no. PB7TO7B04812, Lodz 2000 (in Polish).

[4] Jędral W.: *Centrifugal impeller pumps*, Warsaw Technical University Publishing House, Warsaw 1996 (in Polish).

[5] Kazimierski Z.: *Numerical determination of turbulent flows*, Ossolineum, Wrocław 1992 (in Polish).

[6] Papierski A., Rabiega M.: *Multiblock parallel computation of an incompressible 3-D flow in turbomachines*, TASK Quarterly **3** (1999), No. 1, 39-52 (in Polish).

[7] Papierski A.: *Numerical investigations of the 3D flow structure in centrifugal pumps by means of the domain decomposition method*, PhD Thesis, Lodz 2002 (in Polish).

[8] Rabiega M., Kazimierski Z.: *3-D gas flow through rotating channels – an elliptic approach*, Scientific Bulletin of TUL, Cieplne Maszyny Przepływowe – Turbomachinery (1995), No. 109, 131-141.